# Search for pair production of heavy objects in 4-jets events at $\sqrt{s} = $ 130-136 GeV

W. Adam, T. Adye, E. Agasi, I. Ajinenko, G D. Alekseev, R. Alemany, P P. Allport, S. Almehed, S. Amato, A. Andreazza, et al.

# Search for Pair Production of Heavy Objects in 4-Jet Events at $\sqrt{s} = 130 - 136$ GeV

DELPHI Collaboration

## Abstract

Results are presented of a search for pair production of heavy objects decaying into four hadronic jets, as expected for example from associated or pair production of MSSM Higgs bosons, hA or H$^+$H$^-$, using a data sample of 5.9 pb$^{-1}$ of $e^+e^-$ collisions at $\sqrt{s} = 130 - 136$ GeV collected with the DELPHI detector at LEP in November 1995. The data and expectations from standard processes agree after four-jet selections. An analysis based on $b$-tagging finds no hA candidate with high mass. A study optimized to search for H$^+$H$^-$ events with mass in the $40 - 50$ GeV/$c^2$ range also finds no candidate. Finally a comparison is made with a recent ALEPH analysis which found an excess of four-jet events with high multiplicity and high mass. Such a signal is not observed in the DELPHI data, although a slight excess in the mass region around 105 GeV/$c^2$ is seen.

W.Adam[50], T.Adye[37], E.Agasi[31], I.Ajinenko[42], G.D.Alekseev[16], R.Alemany[49], P.P.Allport[22], S.Almehed[24], U.Amaldi[9], S.Amato[47], A.Andreazza[28], M.L.Andrieux[14], P.Antilogus[9], W-D.Apel[17], B.Åsman[44], J-E.Augustin[25], A.Augustinus[9], P.Baillon[9], P.Bambade[19], F.Barao[21], R.Barate[14], M.Barbi[47], G.Barbiellini[46], D.Y.Bardin[16], A.Baroncelli[40], O.Barring[24], J.A.Barrio[26], W.Bartl[50], M.J.Bates[37], M.Battaglia[15], M.Baubillier[23], J.Baudot[39], K-H.Becks[52], M.Begalli[6], P.Beilliere[8], Yu.Belokopytov[9,53], K.Belous[42], A.C.Benvenuti[5], M.Berggren[47], D.Bertini[25], D.Bertrand[2], M.Besancon[39], F.Bianchi[45], M.Bigi[45], M.S.Bilenky[16], P.Billoir[23], D.Bloch[10], M.Blume[52], T.Bolognese[39], M.Bonesini[28], W.Bonivento[28], P.S.L.Booth[22], G.Borisov[39,42], C.Bosio[40], O.Botner[48], E.Boudinov[31], B.Bouquet[19], C.Bourdarios[9], T.J.V.Bowcock[22], M.Bozzo[13], P.Branchini[40], K.D.Brand[36], T.Brenke[52], R.A.Brenner[15], C.Bricman[2], R.C.A.Brown[9], P.Bruckman[18], J-M.Brunet[8], L.Bugge[33], T.Buran[33], T.Burgsmueller[52], P.Buschmann[52], A.Buys[9], S.Cabrera[49], M.Caccia[28], M.Calvi[28], A.J.Camacho Rozas[41], T.Camporesi[9], V.Canale[38], M.Canepa[13], K.Cankocak[44], F.Cao[2], F.Carena[9], L.Carroll[22], C.Caso[13], M.V.Castillo Gimenez[49], A.Cattai[9], F.R.Cavallo[5], V.Chabaud[9], Ph.Charpentier[9], L.Chaussard[25], P.Checchia[36], G.A.Chelkov[16], M.Chen[2], R.Chierici[45], P.Chliapnikov[42], P.Chochula[7], V.Chorowicz[9], J.Chudoba[30], V.Cindro[43], P.Collins[9], J.L.Contreras[19], R.Contri[13], E.Cortina[49], G.Cosme[19], F.Cossutti[46], J-H.Cowell[22], H.B.Crawley[1], D.Crennell[37], G.Crosetti[13], J.Cuevas Maestro[34], S.Czellar[15], E.Dahl-Jensen[29], J.Dahm[52], B.Dalmagne[19], M.Dam[29], G.Damgaard[29], P.D.Dauncey[37], M.Davenport[9], W.Da Silva[23], C.Defoix[8], A.Deghorain[2], G.Della Ricca[46], P.Delpierre[27], N.Demaria[35], A.De Angelis[9], W.De Boer[17], S.De Brabandere[2], C.De Clercq[2], C.De La Vaissiere[23], B.De Lotto[46], A.De Min[36], L.De Paula[47], C.De Saint-Jean[39], H.Dijkstra[9], L.Di Ciaccio[38], A.Di Diodato[38], F.Djama[10], J.Dolbeau[8], M.Donszelmann[9], K.Doroba[51], M.Dracos[10], J.Drees[52], K.-A.Drees[52], M.Dris[32], J-D.Durand[25], D.Edsall[1], R.Ehret[17], G.Eigen[4], T.Ekelof[48], G.Ekspong[44], M.Elsing[52], J-P.Engel[10], B.Erzen[43], M.Espirito Santo[21], E.Falk[24], D.Fassouliotis[32], M.Feindt[9], A.Ferrer[49], S.Fichet[23], T.A.Filippas[32], A.Firestone[1], P.-A.Fischer[10], H.Foeth[9], E.Fokitis[32], F.Fontanelli[13], F.Formenti[9], B.Franek[37], P.Frenkiel[8], D.C.Fries[17], A.G.Frodesen[4], F.Fulda-Quenzer[19], J.Fuster[49], A.Galloni[22], D.Gamba[45], M.Gandelman[6], C.Garcia[49], J.Garcia[41], C.Gaspar[9], U.Gasparini[36], Ph.Gavillet[9], E.N.Gazis[32], D.Gele[10], J-P.Gerber[10], R.Gokieli[51], B.Golob[43], G.Gopal[37], L.Gorn[1], M.Gorski[51], Yu.Gouz[45,53], V.Gracco[13], E.Graziani[40], C.Green[22], A.Grefrath[52], P.Gris[39], G.Grosdidier[19], K.Grzelak[51], S.Gumenyuk[28,53], P.Gunnarsson[44], M.Gunther[48], J.Guy[37], F.Hahn[9], S.Hahn[52], Z.Hajduk[18], A.Hallgren[48], K.Hamacher[52], W.Hao[31], F.J.Harris[35], V.Hedberg[24], R.Henriques[21], J.J.Hernandez[49], P.Herquet[2], H.Herr[9], T.L.Hessing[35], E.Higon[49], H.J.Hilke[9], T.S.Hill[1], S-O.Holmgren[44], P.J.Holt[35], D.Holthuizen[31], S.Hoorelbeke[2], M.Houlden[22], J.Hrubec[50], K.Huet[2], K.Hultqvist[44], J.N.Jackson[22], R.Jacobsson[44], P.Jalocha[18], R.Janik[7], Ch.Jarlskog[24], G.Jarlskog[24], P.Jarry[39], B.Jean-Marie[19], E.K.Johansson[44], L.Jonsson[24], P.Jonsson[24], C.Joram[9], P.Juillot[10], M.Kaiser[17], F.Kapusta[23], K.Karafasoulis[11], M.Karlsson[44], E.Karvelas[11], S.Katsanevas[3], E.C.Katsoufis[32], R.Keranen[4], Yu.Khokhlov[42], B.A.Khomenko[16], N.N.Khovanski[16], B.King[22], N.J.Kjaer[29], O.Klapp[52], H.Klein[9], A.Klovning[4], P.Kluit[31], B.Koene[31], P.Kokkinias[11], M.Koratzinos[9], K.Korcyl[18], V.Kostioukhine[42], C.Kourkoumelis[3], O.Kouznetsov[13,16], M.Krammer[50], C.Kreuter[17], I.Kronkvist[24], Z.Krumstein[16], W.Krupinski[18], P.Kubinec[7], W.Kucewicz[18], K.Kurvinen[15], C.Lacasta[49], I.Laktineh[25], J.W.Lamsa[1], L.Lanceri[46], D.W.Lane[1], P.Langefeld[52], V.Lapin[42], J-P.Laugier[39], R.Lauhakangas[15], G.Leder[50], F.Ledroit[14], V.Lefebure[2], C.K.Legan[1], R.Leitner[30], J.Lemonne[2], G.Lenzen[52], V.Lepeltier[19], T.Lesiak[18], J.Libby[35], D.Liko[50], R.Lindner[52], A.Lipniacka[44], I.Lippi[36], B.Loerstad[24], J.G.Loken[35], J.M.Lopez[41], D.Loukas[11], P.Lutz[39], L.Lyons[35], J.MacNaughton[50], G.Maehlum[17], J.R.Mahon[6], A.Maio[21], T.G.M.Malmgren[44], V.Malychev[16], F.Mandl[50], J.Marco[41], R.Marco[41], B.Marechal[47], M.Margoni[36], J-C.Marin[9], C.Mariotti[40], A.Markou[11], C.Martinez-Rivero[41], F.Martinez-Vidal[49], S.Marti i Garcia[22], J.Masik[30], F.Matorras[41], C.Matteuzzi[28], G.Matthiae[38], M.Mazzucato[36], M.Mc Cubbin[9], R.Mc Kay[1], R.Mc Nulty[22], J.Medbo[48], M.Merk[31], C.Meroni[28], S.Meyer[17], W.T.Meyer[1], A.Miagkov[42], M.Michelotto[36], E.Migliore[45], L.Mirabito[25], W.A.Mitaroff[50], U.Mjoernmark[24], T.Moa[44], R.Moeller[29], K.Moenig[52], M.R.Monge[13], P.Morettini[13], H.Mueller[17], L.M.Mundim[6], W.J.Murray[37], B.Muryn[18], G.Myatt[35], F.Naraghi[14], F.L.Navarria[5], S.Navas[49], K.Nawrocki[51], P.Negri[28], S.Nemecek[12], W.Neumann[52], N.Neumeister[50], R.Nicolaidou[3], B.S.Nielsen[29], M.Nieuwenhuizen[31], V.Nikolaenko[10], P.Niss[44], A.Nomerotski[36], A.Normand[35], W.Oberschulte-Beckmann[17], V.Obraztsov[42], A.G.Olshevski[16], A.Onofre[21], R.Orava[15], K.Osterberg[15], A.Ouraou[39], P.Paganini[19], M.Paganoni[9,28], P.Pages[10], R.Pain[23], H.Palka[18], Th.D.Papadopoulou[32], K.Papageorgiou[11], L.Pape[9], C.Parkes[35], F.Parodi[13], A.Passeri[40], M.Pegoraro[36], L.Peralta[21], H.Pernegger[50], M.Pernicka[50], A.Perrotta[5], C.Petridou[46], A.Petrolini[13], M.Petrovyck[42], H.T.Phillips[37], G.Piana[13], F.Pierre[39], M.Pimenta[21], S.Plaszczynski[19], O.Podobrin[17], M.E.Pol[6], G.Polok[18], P.Poropat[46], V.Pozdniakov[16], P.Privitera[38], N.Pukhaeva[16], A.Pullia[28], D.Radojicic[35], S.Ragazzi[28], H.Rahmani[32], P.N.Ratoff[20], A.L.Read[33], M.Reale[52], P.Rebecchi[19], N.G.Redaelli[28], M.Regler[50], D.Reid[9], P.B.Renton[35], L.K.Resvanis[3], F.Richard[19], J.Richardson[22], J.Ridky[12], G.Rinaudo[45], I.Ripp[39], A.Romero[45], I.Roncagliolo[13], P.Ronchese[36], L.Roos[14], E.I.Rosenberg[1], E.Rosso[9], P.Roudeau[19], T.Rovelli[5], W.Ruckstuhl[31], V.Ruhlmann-Kleider[39], A.Ruiz[41], K.Rybicki[18], H.Saarikko[15], Y.Sacquin[39], A.Sadovsky[16], O.Sahr[14], G.Sajot[14], J.Salt[49], J.Sanchez[26], M.Sannino[13], M.Schimmelpfennig[17], H.Schneider[17], U.Schwickerath[17], M.A.E.Schyns[52], G.Sciolla[45], F.Scuri[46], P.Seager[20], Y.Sedykh[16], A.M.Segar[35], A.Seitz[17], R.Sekulin[37], L.Serbelloni[38], R.C.Shellard[6], I.Siccama[31], P.Siegrist[39], R.Silvestre[39], S.Simonetti[39], F.Simonetto[36], A.N.Sisakian[16], B.Sitar[7], T.B.Skaali[33], G.Smadja[25], N.Smirnov[42], O.Smirnova[24], G.R.Smith[37], A.Sokolov[42], R.Sosnowski[51], D.Souza-Santos[6], T.Spassov[21], E.Spiriti[40], P.Sponholz[52], S.Squarcia[13], C.Stanescu[40], S.Stapnes[33], I.Stavitski[36], K.Stevenson[35], F.Stichelbaut[9],

A.Stocchi[19], J.Strauss[50], R.Strub[10], B.Stugu[4], M.Szczekowski[51], M.Szeptycka[51], T.Tabarelli[28], J.P.Tavernet[23], O.Tchikilev[42], J.Thomas[35], A.Tilquin[27], J.Timmermans[31], L.G.Tkatchev[16], T.Todorov[10], S.Todorova[10], D.Z.Toet[31], A.Tomaradze[2], B.Tome[21], A.Tonazzo[28], L.Tortora[40], G.Transtromer[24], D.Treille[9], W.Trischuk[9], G.Tristram[8], A.Trombini[19], C.Troncon[28], A.Tsirou[9], M-L.Turluer[39], I.A.Tyapkin[16], M.Tyndel[37], S.Tzamarias[22], B.Ueberschaer[52], O.Ullaland[9], V.Uvarov[42], G.Valenti[5], E.Vallazza[9], G.W.Van Apeldoorn[31], P.Van Dam[31], W.K.Van Doninck[2], J.Van Eldik[31], N.Vassilopoulos[35], G.Vegni[28], L.Ventura[36], W.Venus[37], F.Verbeure[2], M.Verlato[36], L.S.Vertogradov[16], D.Vilanova[39], P.Vincent[25], L.Vitale[46], E.Vlasov[42], A.S.Vodopyanov[16], V.Vrba[12], H.Wahlen[52], C.Walck[44], M.Weierstall[52], P.Weilhammer[9], C.Weiser[17], A.M.Wetherell[9], D.Wicke[52], J.H.Wickens[2], M.Wielers[17], G.R.Wilkinson[35], W.S.C.Williams[35], M.Winter[10], M.Witek[18], K.Woschnagg[48], K.Yip[35], O.Yushchenko[42], F.Zach[25], A.Zaitsev[42], A.Zalewska[9], P.Zalewski[51], D.Zavrtanik[43], E.Zevgolatakos[11], N.I.Zimin[16], M.Zito[39], D.Zontar[43], G.C.Zucchelli[44], G.Zumerle[36]

[1] Department of Physics and Astronomy, Iowa State University, Ames IA 50011-3160, USA
[2] Physics Department, Univ. Instelling Antwerpen, Universiteitsplein 1, B-2610 Wilrijk, Belgium
and IIHE, ULB-VUB, Pleinlaan 2, B-1050 Brussels, Belgium
and Faculté des Sciences, Univ. de l'Etat Mons, Av. Maistriau 19, B-7000 Mons, Belgium
[3] Physics Laboratory, University of Athens, Solonos Str. 104, GR-10680 Athens, Greece
[4] Department of Physics, University of Bergen, Allégaten 55, N-5007 Bergen, Norway
[5] Dipartimento di Fisica, Università di Bologna and INFN, Via Irnerio 46, I-40126 Bologna, Italy
[6] Centro Brasileiro de Pesquisas Físicas, rua Xavier Sigaud 150, RJ-22290 Rio de Janeiro, Brazil
and Depto. de Física, Pont. Univ. Católica, C.P. 38071 RJ-22453 Rio de Janeiro, Brazil
and Inst. de Física, Univ. Estadual do Rio de Janeiro, rua São Francisco Xavier 524, Rio de Janeiro, Brazil
[7] Comenius University, Faculty of Mathematics and Physics, Mlynska Dolina, SK-84215 Bratislava, Slovakia
[8] Collège de France, Lab. de Physique Corpusculaire, IN2P3-CNRS, F-75231 Paris Cedex 05, France
[9] CERN, CH-1211 Geneva 23, Switzerland
[10] Centre de Recherche Nucléaire, IN2P3 - CNRS/ULP - BP20, F-67037 Strasbourg Cedex, France
[11] Institute of Nuclear Physics, N.C.S.R. Demokritos, P.O. Box 60228, GR-15310 Athens, Greece
[12] FZU, Inst. of Physics of the C.A.S. High Energy Physics Division, Na Slovance 2, 180 40, Praha 8, Czech Republic
[13] Dipartimento di Fisica, Università di Genova and INFN, Via Dodecaneso 33, I-16146 Genova, Italy
[14] Institut des Sciences Nucléaires, IN2P3-CNRS, Université de Grenoble 1, F-38026 Grenoble Cedex, France
[15] Research Institute for High Energy Physics, SEFT, P.O. Box 9, FIN-00014 Helsinki, Finland
[16] Joint Institute for Nuclear Research, Dubna, Head Post Office, P.O. Box 79, 101 000 Moscow, Russian Federation
[17] Institut für Experimentelle Kernphysik, Universität Karlsruhe, Postfach 6980, D-76128 Karlsruhe, Germany
[18] Institute of Nuclear Physics and University of Mining and Metalurgy, Ul. Kawiory 26a, PL-30055 Krakow, Poland
[19] Université de Paris-Sud, Lab. de l'Accélérateur Linéaire, IN2P3-CNRS, Bât. 200, F-91405 Orsay Cedex, France
[20] School of Physics and Chemistry, University of Lancaster, Lancaster LA1 4YB, UK
[21] LIP, IST, FCUL - Av. Elias Garcia, 14-1°, P-1000 Lisboa Codex, Portugal
[22] Department of Physics, University of Liverpool, P.O. Box 147, Liverpool L69 3BX, UK
[23] LPNHE, IN2P3-CNRS, Universités Paris VI et VII, Tour 33 (RdC), 4 place Jussieu, F-75252 Paris Cedex 05, France
[24] Department of Physics, University of Lund, Sölvegatan 14, S-22363 Lund, Sweden
[25] Université Claude Bernard de Lyon, IPNL, IN2P3-CNRS, F-69622 Villeurbanne Cedex, France
[26] Universidad Complutense, Avda. Complutense s/n, E-28040 Madrid, Spain
[27] Univ. d'Aix - Marseille II - CPP, IN2P3-CNRS, F-13288 Marseille Cedex 09, France
[28] Dipartimento di Fisica, Università di Milano and INFN, Via Celoria 16, I-20133 Milan, Italy
[29] Niels Bohr Institute, Blegdamsvej 17, DK-2100 Copenhagen 0, Denmark
[30] NC, Nuclear Centre of MFF, Charles University, Areal MFF, V Holesovickach 2, 180 00, Praha 8, Czech Republic
[31] NIKHEF, Postbus 41882, NL-1009 DB Amsterdam, The Netherlands
[32] National Technical University, Physics Department, Zografou Campus, GR-15773 Athens, Greece
[33] Physics Department, University of Oslo, Blindern, N-1000 Oslo 3, Norway
[34] Dpto. Fisica, Univ. Oviedo, C/P. Pérez Casas, S/N-33006 Oviedo, Spain
[35] Department of Physics, University of Oxford, Keble Road, Oxford OX1 3RH, UK
[36] Dipartimento di Fisica, Università di Padova and INFN, Via Marzolo 8, I-35131 Padua, Italy
[37] Rutherford Appleton Laboratory, Chilton, Didcot OX11 OQX, UK
[38] Dipartimento di Fisica, Università di Roma II and INFN, Tor Vergata, I-00173 Rome, Italy
[39] CEA, DAPNIA/Service de Physique des Particules, CE-Saclay, F-91191 Gif-sur-Yvette Cedex, France
[40] Istituto Superiore di Sanità, Ist. Naz. di Fisica Nucl. (INFN), Viale Regina Elena 299, I-00161 Rome, Italy
[41] Instituto de Fisica de Cantabria (CSIC-UC), Avda. los Castros, S/N-39006 Santander, Spain, (CICYT-AEN93-0832)
[42] Inst. for High Energy Physics, Serpukov P.O. Box 35, Protvino, (Moscow Region), Russian Federation
[43] J. Stefan Institute and Department of Physics, University of Ljubljana, Jamova 39, SI-61000 Ljubljana, Slovenia
[44] Fysikum, Stockholm University, Box 6730, S-113 85 Stockholm, Sweden
[45] Dipartimento di Fisica Sperimentale, Università di Torino and INFN, Via P. Giuria 1, I-10125 Turin, Italy
[46] Dipartimento di Fisica, Università di Trieste and INFN, Via A. Valerio 2, I-34127 Trieste, Italy
and Istituto di Fisica, Università di Udine, I-33100 Udine, Italy
[47] Univ. Federal do Rio de Janeiro, C.P. 68528 Cidade Univ., Ilha do Fundão BR-21945-970 Rio de Janeiro, Brazil
[48] Department of Radiation Sciences, University of Uppsala, P.O. Box 535, S-751 21 Uppsala, Sweden
[49] IFIC, Valencia-CSIC, and D.F.A.M.N., U. de Valencia, Avda. Dr. Moliner 50, E-46100 Burjassot (Valencia), Spain
[50] Institut für Hochenergiephysik, Österr. Akad. d. Wissensch., Nikolsdorfergasse 18, A-1050 Vienna, Austria
[51] Inst. Nuclear Studies and University of Warsaw, Ul. Hoza 69, PL-00681 Warsaw, Poland
[52] Fachbereich Physik, University of Wuppertal, Postfach 100 127, D-42097 Wuppertal, Germany
[53] On leave of absence from IHEP Serpukhov

# 1   Introduction

During the data taking at LEP in November 1995, events at centre-of-mass energies of 130 and 136 GeV were recorded by the DELPHI detector, with a total integrated luminosity of 5.9 pb$^{-1}$.

This allows a search for new physics at higher mass in the four-jet channel, mainly the possible production in pairs of the Higgs bosons, hA and H$^+$H$^-$, predicted by the Minimal Supersymmetric extension of the Standard Model (MSSM).

For the hA channel, given the high branching ratios of these Higgs bosons to quarks (more than 90% to $b\bar{b}$), the final topology expected consists of four hadronic jets and no missing energy. Additional signatures are given by the $b$ content of the jets and by the peak expected in the di-jet mass distribution. Previous limits from DELPHI at LEP1 [1] allow this hA search to be restricted to $m_{\rm h}$ above 44 GeV/$c^2$ for any value of the MSSM parameter $\tan\beta$, and $m_{\rm A}$ above 39 GeV/$c^2$ for $\tan\beta$ above 1.

Four-jet events are also expected in the H$^+$H$^-$ channel for low values of $\tan\beta$, where the branching ratio for H$^+$ to $c\bar{s}$ is high. In this case, a constraint on the equality of the two masses can be applied to reduce the background. Previous limits obtained by DELPHI at LEP1 [2] allow this search to be limited to masses above 43.5 GeV/$c^2$.

Additional interest in this type of event comes from the excess of four-jet events with a sum of two di-jet masses around 105 GeV/$c^2$, found by the ALEPH collaboration [3] after cuts based on the mass and multiplicity of the jets.

The next section summarises the features of the DELPHI detector relevant to this analysis. Section 3 describes the event selection, the jet reconstruction, and the mass measurement. Section 4 presents the hA analysis based on $b$-tagging. Section 5 details the search optimized for H$^+$H$^-$ with a boson mass in the range $40-50$ GeV/$c^2$. Finally, the last section describes an analysis made to check the excess reported by the ALEPH collaboration.

# 2   The DELPHI detector and data samples

A detailed description of the DELPHI detector and its performance can be found in references [4,5]. The reconstruction of four-jet events relies on the tracking detectors and calorimeters.

The tracking detectors are the microvertex detector (VD), the inner detector (ID), the time projection chamber (TPC), and the outer detector in the barrel region, and the forward chambers. The ID and TPC cover the polar angles to the beam, $\theta$, between 20° and 160°. Charged particles used in the analysis have a track length of at least 30 cm, a momentum $p$ above 100 MeV/$c$ measured with a relative error $\Delta p/p$ less than one, and a distance of closest approach to the primary vertex smaller than 4 cm in the plane perpendicular to the beam axis and 10 cm along the beam axis.

The barrel and forward electromagnetic calorimeters, HPC and EMF, are used for the electromagnetic energy reconstruction, covering 43° $< \theta <$ 137°, and 10° $< \theta <$ 36.5°, 143.5° $< \theta <$ 170° respectively. The hadron calorimeter, employed to measure the neutral hadronic energy, covers polar angles down to 10° in $\theta$. Neutral clusters kept in the analysis have a minimum energy of 200 MeV.

The rejection of radiative events makes use of the STIC (small angle tile calorimeter), covering the region 1.66° $< \theta <$ 10.6°, 169.4° $< \theta <$ 178.34°.

The probability of the presence of beauty hadrons in jets is given by $b$-tag algorithms, based on the use of the double-sided microvertex detector [6], with a polar angle coverage $44° < \theta < 136°$.

The data sample was collected by DELPHI at LEP during November 1995. The integrated luminosities accumulated were 2.92 pb$^{-1}$ and 3.01 pb$^{-1}$ at centre-of-mass energies of 130.4 GeV and 136.3 GeV respectively.

Detector effects on the analysis were studied using DELSIM [5], the full simulation program of DELPHI. Events were generated with the JETSET 7.4 / PYTHIA 5.7 Parton Shower (PS) model [7] with parameters tuned by DELPHI, and with the DYMU3 generator [8] (including double initial state radiation). The particles were followed through the detailed geometry of DELPHI giving simulated digitisations in each detector. These data were processed with the same reconstruction and analysis programs as the real data.

A four-jet signal sample of hA events generated with PYTHIA in which both h and A had masses equal to 55 GeV/$c^2$ and zero widths was fully simulated, and also samples of H$^+$H$^-$ events with $m_{\mathrm{H}\pm} = 44\,\mathrm{GeV}/c^2$ and $46\,\mathrm{GeV}/c^2$.

The corresponding background processes are mainly QCD events, namely $e^+e^- \to q\bar{q}$ events giving four jets after gluon radiation ($q\bar{q}gg$ and $q\bar{q}q'\bar{q}'$). A much smaller contribution at these centre-of-mass energies is expected from ZZ and WW events, and a marginal one from $\gamma\gamma$ processes or Bhabha events.

Table 1 shows the expected cross-sections, and the statistics of simulated events employed in the analysis.

# 3    Selection of four-jet events

## 3.1    Preselection of events

The selection procedure is based on the expected signature: non-radiative hadronic events with no missing energy and giving four hadronic jets.

Hadronic events were selected by requiring at least 10 charged particles with momentum above 200 MeV/$c$ and a total energy exceeding $0.12 \times E_{\mathrm{cms}}$. The total electromagnetic energy of the event was required to be below 90 GeV, to reject a few remaining Bhabha events, and the total charged particle energy above 50 GeV, to eliminate the $\gamma\gamma$ background without affecting the signal.

Many of these events are radiative $q\bar{q}\gamma$ events, either with an initial state radiation (ISR) photon seen either in the STIC or in the EMF, or with an undetected one aligned along the beam. In this last case the missing photon energy was computed from energy and momentum conservation, after clustering the event into two jets and assuming a photon collinear to the beam axis. Events with a photon of more than 20 GeV, seen with an isolation angle of at least 15° or else invisible, were then rejected as radiative.

A total of 672 events were selected in the data after these preliminary cuts, while 653± 5 (stat. only) are expected from the background simulation. The efficiency of this selection for a four-jet signal is 94%.

## 3.2    Jet reconstruction

The jet structure of the selected hadronic events was then studied with a clusterizing algorithm like DURHAM [9] or JADE [10] (similar results were obtained with both algorithms when applied to a four-jet signal).

For the preselection of events, the DURHAM algorithm was employed, with a low $y_{cut}$ value of 0.003 to minimize the loss of signal efficiency. Events with less than four jets were rejected, while those retained were forced to a four-jet configuration by raising the $y_{cut}$ value. The jets were required to be hadronic-like by demanding at least two charged particles per jet and that at most 80% of their energy was electromagnetic (i.e. was measured in the HPC, EMF or STIC).

A total of 95 four-jet events were selected in the data, while $98 \pm 3$ are expected from standard processes. The efficiency for the four-jet signal at this level was 81%.

## 3.3    Mass measurement

The most direct signature for a pair of new heavy objects is the measurement of their masses, which relies on the jet reconstruction. Since the jet directions are measured more precisely than their energies, a simple rescaling method is used based on total energy and momentum conservation:

$$\sum \vec{\beta}_i E_i = \vec{0},$$

$$\sum E_i = E_{cm},$$

with $E_i = k_i E_i^m$ and $\vec{\beta}_i = \vec{p}_i^m / E_i^m$, where the suffix $m$ denotes the measured values of the jet energy and momentum, and $k_i$ is the rescaling factor for jet $i$ and is determined from the above equations, and has to be positive. This improves the mass measurements and also rejects some badly measured events, and some residual radiative events, returning negative rescaling factors.

After this rescaling, 64 events were found in the data, while $62 \pm 2$ are expected. The efficiency for the hA signal was 75%. Table 2 summarises the preselection of the four-jet events.

The rescaling method gives its best resolution on the sum of the di-jet masses, $\Sigma M$. There are three possible combinations of di-jets, 12-34, 13-24, and 14-23. If the jets are ordered in energy, 1 being the most energetic, simulation shows that, for masses in the interesting range, the 12-34 combination is very unlikely and the best efficiency for a four-jet signal is obtained with the combination 13-24 or 14-23 giving the smallest di-jet mass difference, $\Delta M$.

The resolution $\sigma_{\Sigma M}$ on the di-jet mass sum expected for a four-jet signal with $m_h = m_A = 55$ GeV/$c^2$ and zero widths, at 130 and 136 GeV, is around 1.9 GeV/$c^2$. The corresponding di-jet mass difference $\Delta M$ is measured with a worse resolution, $\sigma_{\Delta M} = 7$ GeV/$c^2$. This behaviour results from the energy constraint applied in the rescaling and the high value of the di-jet mass sum.

# 4    Search for hA events using $b$-tag

The MSSM predicts the associated production of the neutral Higgs bosons, hA, both decaying predominantly to a $b\bar{b}$ pair, so giving a $b\bar{b}b\bar{b}$ final state in 83% of cases, with a cross-section depending on the model parameters:

$$\sigma_{hA} = \frac{1}{2} \lambda^3 \left(1, \frac{m_h^2}{s}, \frac{m_A^2}{s}\right) \cos^2(\alpha - \beta) \, \sigma_{\nu\bar{\nu}},$$

where $\alpha$ is the mixing angle, $\sigma_{\nu\bar{\nu}}$ is the cross-section for $e^+e^- \to Z \to \nu\bar{\nu}$ for one neutrino family at $s = E_{\mathrm{cms}}^2$, and $\lambda$ is the phase space factor:

$$\lambda(x, y, z) = \sqrt{(x - y - z)^2 - 4yz}\,.$$

At these centre-of-mass energies, this cross-section is significant for the newly accessible mass range only if $\tan\beta$ is high: for example for $\tan\beta = 20$ and $m_{\mathrm{A}} = 55$ GeV$/c^2$, $\sigma_{\mathrm{hA}} = 0.4$ pb at $E_{\mathrm{cms}} = 136$ GeV. In this case both Higgs masses would be practically equal, and have a sizeable width (of the order of 0.6 GeV).

The search relied on $b$-tagging techniques to suppress the QCD, WW and ZZ backgrounds. This $b$-tagging is based on the impact parameters of charged particles measured using the microvertex detector (VD). The method [11] counts offsets in $r\phi$ and $z$, defined as charged particles with a momentum of at least 0.5 GeV$/c^2$, at least two $r\phi$ hits [†] and one $z$ hit (two for $z$ offsets) associated in the VD, and with a positive lifetime-signed impact parameter in $r\phi$ or $z$ larger than 2.5 times its error.

Two levels of $b$-tag were applied to the events previously selected.

- The loose $b$-tag requests five or more offsets in the event (a cut employed to select $b\bar{b}$ events): 16 events passed this cut, while 11 are expected according to the background simulation; the signal efficiency was still around 70%.
- The tighter cut requests 3 of the 4 jets to have at least two offsets (either in $r\phi$ or $z$). This cut was used to suppress the main source of background, $b\bar{b}gg$ events.

Fig. 1 shows the mass distribution without $b$-tag, with loose $b$-tag and with tight $b$-tag for data, simulated background, and an hA -like signal corresponding to four times the DELPHI luminosity.

After the tighter cut only one event was left in the data, while 1.3 are expected from the background simulation. The signal efficiency was 46%.

This event has a sum of di-jet masses equal to 66 GeV$/c^2$ and a difference of di-jet masses of 22 GeV$/c^2$. So the interesting region ($m_{\mathrm{A}} > 40$ GeV$/c^2$) contains no candidate.

This result can be translated into a 95% confidence level (CL) upper limit on the cross-section of 1.3 pb, which gives no improvement with respect to LEP1. However, the combined statistics of the four LEP experiments could give sensitivity to cross-sections of order 0.33 pb, corresponding to an exclusion limit at 95% CL of $m_{\mathrm{A}} > 57$ GeV$/c^2$ in the high $\tan\beta$ region of the ($m_{\mathrm{A}}$, $\tan\beta$) plane.

# 5   Search for $\mathrm{H^+H^-}$

In $e^+e^-$ interactions, charged Higgs bosons are predicted to be pair-produced via $s$-channel $\gamma$ and Z exchanges. The tree-level cross-section, which depends only on $m_{\mathrm{H+}}$, is given by the following expression [12]:

$$\sigma_0 \;=\; \frac{1}{4}\,\sigma_{\mu^+\mu^-}\,\beta_{\mathrm{H}}^3\left(1 - \frac{2C_V C_V'\,s(s - m_Z^2)}{(s - m_Z^2)^2 + m_Z^2\Gamma_Z^2} + \frac{C_V'^2(C_V^2 + C_A^2)\,s^2}{(s - m_Z^2)^2 + m_Z^2\Gamma_Z^2}\right).$$

Here $\sigma_{\mu^+\mu^-} = 4\pi\alpha_{em}^2/3s$, $\beta_{\mathrm{H}} = (1 - 4m_{\mathrm{H}\pm}^2/s)^{1/2}$ is the charged Higgs boson velocity, the rescaled Z charges are defined by $C_V = (1 - 4\sin^2\theta_{\mathrm{W}})/4\sin\theta_{\mathrm{W}}\cos\theta_{\mathrm{W}}$, $C_A = -1/4\sin\theta_{\mathrm{W}}\cos\theta_{\mathrm{W}}$, and $C_V' = (-1 + 2\sin^2\theta_{\mathrm{W}})/2\sin\theta_{\mathrm{W}}\cos\theta_{\mathrm{W}}$. In all expressions, $\alpha_{em}$ is

---

[†]Relative to the beam direction, $z$ is measured longitudinally, $r$ radially, and $r\phi$ transversely.

the electromagnetic coupling constant, $\theta_W$ is the electroweak mixing angle, and $\sqrt{s}$ is the centre-of-mass energy.

Taking account of radiative corrections (ie photon radiation and vertex corrections), the total cross-section is predicted to be 1.03 pb for $m_{H^+} = 44\,\text{GeV}/c^2$, decreasing to 0.32 pb for $m_{H^+} = 55\,\text{GeV}/c^2$. Such low values (compared to the production cross-sections of other particles of the MSSM, such as charginos) require a large integrated luminosity to exclude a signal at the 95% confidence level. With 5.9 p$b^{-1}$, one can expect to exclude only at the one standard deviation level, and only for masses lower than $50\,\text{GeV}/c^2$.

For these masses the only possible decays are into fermion pairs. In any two-doublet model, the width of these decays is proportional to the squared mass of the fermions, and to a squared CKM matrix element when the fermions are quarks. Therefore, the process $H^+ \rightarrow \tau^+ \bar{\nu}_\tau$ is dominant among leptonic decays, and $H^+ \rightarrow c\bar{s}$ is dominant among hadronic decays, $H^+ \rightarrow c\bar{b}$ being suppressed by the small value of $V_{cb}$. Within the MSSM, the relative amount of leptonic decays, compared to hadronic decays, is fixed by the value of $\tan\beta$ : for high values of this parameter ($\tan\beta > 5.0$), the leptonic decay is dominant. In the present analysis, we assume that the two bosons decay into hadrons, and search for a four-jet topology without missing energy.

In order to optimize the search, a linear function $F$ of measured shape and jet variables was built, following the Fisher discriminant analysis method [13]. This function discriminated between a simulated charged Higgs boson signal sample with a mass of $44\,\text{GeV}/c^2$ (representing the first class of population of variables), and a simulated $f\bar{f}(n\gamma)$ background sample (representing the second class of population of variables). The events of these samples had to pass the hadronic preselection cuts described in the first paragraph of section 3.1. $F$ was calculated by maximizing the ratio of between-class variance to the within-class variance. It was found to be a combination of the following variables :

- $\mathcal{J}$, a variable defined as $\min_j(E_j) \times \min_{ik}(\alpha_{ik})$, the product of the energy of the least energetic jet (in GeV) and the minimum opening angle between any two jets (in radians): this measures the quality of the separation between any pair of jets, once the event has been forced to be a four-jet event with the JADE algorithm;
- $\mathcal{T}$, the event *thrust*;
- $|\cos(\theta_{sph})|$, where $\theta_{sph}$ is the polar angle of the *sphericity* axis which is strongly correlated to the polar angle $\theta^*$ of the produced $H^+$ and enables us to exploit the fact that, for pair-produced scalars, the differential cross-section is proportional to $\sin^2\theta^*$.

The linear combination was : $F = -0.136 \times \mathcal{J} + 11.6 \times \mathcal{T} + 1.37 \times |\cos(\theta_{sph})|$. Fig. 2 shows the distribution of $F$ for real and simulated data at the hadronic preselection level and at the four-jet selection level. The requirement $F \leq 8.55$ keeps a high signal efficiency while rejecting most of the background.

After applying this cut at the level of the four-jet selection described in section 3 (after rescaling), 11 events were selected in the real data, while $13.2 \pm 0.8$ were expected from simulated $f\bar{f}(n\gamma)$. The efficiency for the signal was found to be 37% ($m_{H^+} = 44\,\text{GeV}/c^2$ sample).

A kinematic fit was then applied [14], which constrained the measured energies and angles of the jets to satisfy conservation of total energy and momentum and equality between the invariant masses of the two chosen jet pairs, chosen as described in section 3.3. Events were kept if the overall $\chi^2$ of the fit was lower than 25 (for the signal, before this cut, the $\chi^2$ had a mean value of 10). With this cut, 7 events were selected while expecting $10.6 \pm 0.8$ from the simulated background.

Further cuts were applied on the value of the jet pair invariant mass (the reconstructed $H^+$ mass) and on the value of the minimal angle between the fitted momenta of the jets. This last variable can discriminate signal events from background events where two jets resulting from the hadronisation of a quark and of a radiated gluon are frequently close to each other. The cuts used (see Fig. 3) were fixed in order to keep the best efficiency for two signal samples, with $m_{H+} = 44\,\mathrm{GeV}/c^2$ and $46\,\mathrm{GeV}/c^2$. No events were selected, while $2.4 \pm 0.4$ were expected from the simulated $f\bar{f}(n\gamma)$sample. The final efficiency of the signal was found to be 29%.

The LEP1 result on the charged Higgs boson mass is not changed : only a one standard deviation exclusion curve can be obtained from these results in the $[m_{H+}, BR(H^+ \to hadrons)]$ plane, and that only for masses lower than $47.5\,\mathrm{GeV}/c^2$ (see Fig. 4).

# 6    Analysis motivated by the ALEPH excess

The ALEPH Collaboration has reported [3] an excess of four-jet events observed at $\sqrt{s} = 130 - 136$ GeV, with respect to the standard model predictions.

Their analysis, originally oriented towards the hA search, starts with a four-jet topology selection similar to the one applied in DELPHI, but with a higher value for $y_{cut}$, 0.008. They also recover events which the DURHAM algorithm reconstructs with less than four jets, using the JADE algorithm with a $y_{cut}$ value of 0.022 to increase by 10% the final efficiency for a four-jet signal.

Then three cuts are applied to reduce the QCD and four-fermion background, requiring large di-jet masses, large jet masses and large multiplicities. The first cut requires that all di-jet masses exceed $25\,\mathrm{GeV}/c^2$; the second one that the sum of the masses of the two lightest jets is larger than $10\,\mathrm{GeV}/c^2$; and the last one that the sum of their charged multiplicity is at least 10.

This analysis has been adapted to DELPHI, taking into account the differences in tracking efficiency and in detector coverage. In particular, applying the ALEPH analysis directly to DELPHI data does not suppress the radiative returns sufficiently. Additional requirements on the electromagnetic energy of the jets (below 30 GeV in the barrel, 20 GeV in the forward region) and on the rescaling factors (less than 2.0 for the first and second jet, 2.5 for the third jet, 3.0 for the fourth jet) were therefore applied for this purpose. The three ALEPH cuts were then applied, relaxing their values by 10% to maintain the same overall efficiency for hA -like events.

Table 3 shows the result of applying these three cuts to the four-jet events previously selected, and its effect on the simulation samples. Finally, 12 events are selected in the data while $9.8 \pm 0.6$ are expected from standard processes. Using the 44% estimated efficiency for the hA -like signal, a 95% CL upper limit of 3.8 pb on the cross-section of a new channel is derived.

Table 4 shows the sum of di-jet masses for the relevant pairings (13-24 and 14-23). All events have been graphically scanned in detail, the four-jet structure and invariant mass values of these events have been confirmed, and no detector problem has been found.

No statistically significant peak structure is seen in the corresponding mass plot (Fig. 5), although more events than expected have high mass values. Eight events are found with masses between 96 and 120 $\mathrm{GeV}/c^2$ where $3.5 \pm 0.4$ are expected, corresponding to a probability below 5%. Four events are found in the mass range corresponding to the excess observed by ALEPH (102–110 $\mathrm{GeV}/c^2$) where $0.9 \pm 0.1$ are expected.

Fig. 6 shows the bi-dimensional plot of the difference of di-jet masses versus their sum for the chosen combination. Due to the pairing problem, and since the masses of the two heavy objects can be different, the second combination could sometimes be the right one. Fig. 7 shows the bi-dimensional plot of the sum of the di-jet masses for both combinations 13-24 and 14-23 and the projection of both pairings. Good agreement is found between data and the background simulation. The 102–110 GeV/$c^2$ band contains one event more than the single projection seen in Fig. 5. The corresponding plots for an hA -like signal are shown for comparison, and also the projection on to the $\Delta M$ axis.

Fig. 8 shows the distribution of the polar angle of production for the hypothesis of production of a pair of heavy objects, each decaying into a di-jet, for the five possible candidates in the mass range 102–110 GeV/$c^2$, together with the expected distribution from background. Also shown for comparison is the $\sin^2\theta^*$ distribution corresponding to the production of a pair of scalar particles.

Finally, any radiative return candidates that are still hidden can be identified in principle by a recoil mass near $M_Z$ for the jet that originated from the radiated photon, which would more probably also have a low polar angle. The recoil mass is calculated from the centre-of-mass energy and the rescaled jet momentum. Fig. 9 shows the corresponding plot for the selected events.

# 7 Conclusions

The results have been presented of a search for pair production of heavy objects decaying into four hadronic jets, using a data sample of 5.9 pb$^{-1}$ of $e^+e^-$ collisions at $\sqrt{s} = 130 - 136$ GeV collected with the DELPHI detector at LEP in November 1995. Good agreement between data and the expectation from standard processes is found at the four-jet selection level.

The analysis based on $b$-tagging finds no hA candidate with high mass, at an efficiency level of 46%. If the other LEP experiments were to see the same as DELPHI, a new limit on the $A$ mass (of order of 57 GeV/$c^2$ for high $\tan\beta$) could be set.

The study optimized to search for H$^+$H$^-$ events with mass in the 40-50 GeV/$c^2$ range also finds no candidate, while maintaining a 29% efficiency.

Finally, an ALEPH-like analysis, looking for events with four jets with high multiplicity and mass, finds no anomaly, although it does show a slight excess of events in the mass region around 105 GeV/$c^2$. Additional statistics would help to understand its origin.

## Acknowledgements

| process | 130 GeV | | 136 GeV | |
|---|---|---|---|---|
| | $\sigma$ | # events | $\sigma$ | # events |
| $f\bar{f}(\mathrm{n}\gamma)$ | 475 pb | 33700 | 407 pb | 33400 |
| Z/$\gamma^*$ or Z/$\gamma^*$ | 0.5 pb | 60 | 0.5 pb | 60 |
| WW | 0.4 pb | 60 | 0.5 pb | 60 |
| $\gamma\gamma$ | 1330 pb | 10000 | 1480 pb | 10000 |
| Bhabha | 2455 pb | 12500 | 2303 pb | 13600 |
| hA $(m_h = m_A = 55\,\mathrm{GeV}/c^2)$ | 0.37 pb | 214 | 0.40 pb | 208 |
| H$^+$H$^-$ $(m_{H+} = m_{H-} = 44\,\mathrm{GeV}/c^2)$ | 1.03 pb | 800 | 0.98 pb | — |
| H$^+$H$^-$ $(m_{H+} = m_{H-} = 46\,\mathrm{GeV}/c^2)$ | 0.83 pb | 800 | 0.82 pb | — |

Table 1: Expected cross-sections and sizes of the simulation samples used in the analysis

| | observed events | expected events (QCD + ZZ + WW) | simulated signal efficiency |
|---|---|---|---|
| hadronic events with $E_{charged} > 50$ GeV/$c^2$ | 1101 | 1077 $\pm$ 6 | 98% |
| after anti-ISR cuts $E_\gamma \leq 20$ GeV | 672 | 653$\pm$ 5 | 94% |
| four hadronic jets $y_{cut} > 0.003(\mathrm{DURHAM})$ | 95 | 98$\pm$ 3 | 81% |
| positive rescaling | 64 | 62$\pm$ 2 | 75% |

Table 2: Selection of four-jet events

| | observed events | expected events (QCD + ZZ + WW) | signal efficiency |
|---|---|---|---|
| four-jet events with good rescaling $y_{cut} > 0.003$ (DURHAM) or $y_{cut} > 0.01$ (JADE) | 52 | $48 \pm 2$ | 68% |
| $y_{cut} > 0.008$ (DURHAM) or $y_{cut} > 0.022$(JADE) | 25 | $20 \pm 1$ | 57% |
| $\min(M_{ij}^{rec}) > 22.5$ GeV/$c^2$ | 16 | $14.6 \pm 0.7$ | 54% |
| $\min(m_i^{rec} + m_j^{rec}) > 9$ GeV/$c^2$ | 14 | $10.5 \pm 0.6$ | 46% |
| $\min(n_{CHi} + n_{CHj}) \geq 9$ | 12 | $9.8 \pm 0.6$ | 44% |

Table 3: Effects of the ALEPH-like selection cuts

| $\sqrt{s}$ | algorithm | $\Sigma M_{13-24}$ | $\Delta M_{13-24}$ | $\Sigma M_{14-23}$ | $\Delta M_{14-23}$ |
|---|---|---|---|---|---|
| 130 | **JADE** | 104.9 | 27.3 | **98.1** | -24.1 |
| 130 | **JADE** | 120.5 | 5.8 | **64.0** | -2.1 |
| 130 | **DURHAM** | 116.3 | 36.9 | **71.2** | 24.3 |
| 130 | **DURHAM** | 93.2 | 8.6 | **103.6** | 2.8 |
| 136 | **DURHAM** | 120.4 | 18.4 | **124.5** | 6.6 |
| 136 | **DURHAM** | 106.5 | 38.2 | **106.5** | 11.5 |
| 136 | **DURHAM** | 100.8 | 38.5 | **87.0** | 32.7 |
| 136 | **JADE** | 97.9 | 30.2 | **102.7** | -0.1 |
| 136 | **JADE** | 89.0 | 37.1 | **116.6** | 2.8 |
| 136 | **DURHAM** | 115.2 | 54.2 | **83.9** | 11.3 |
| 136 | **JADE** | 96.2 | 31.7 | **103.7** | 25.9 |
| 136 | **JADE** | 62.0 | 8.3 | **110.2** | -4.1 |

Table 4: List of events, indicating their centre-of-mass energies, the clustering algorithm employed, and the sum and difference of the di-jet masses (in GeV/$c^2$) for the two interesting di-jet combinations. In bold, the mass value selected (by taking the pairing with the smaller absolute di-jet mass difference).

# References

[1] DELPHI Collaboration, P. Abreu et al., *Z. Phys.* **C67** (1995) 69.

[2] DELPHI Collaboration, P. Abreu et al., *Z. Phys.* **C64** (1994) 183.

[3] ALEPH Collaboration, CERN PRE 95-003 , "Preliminary results from the 130/136 GeV LEP run with ALEPH", presented by G. Rolandi at CERN Particle Physics Seminar;
ALEPH Collaboration, D. Buskulic et al., "Four-jet final state production in ee collisions at centre of mass energies of 130 and 136 GeV ", CERN-PPE/96-052, subm. to Z. Phys. C;
Preliminary results from the other LEP collaborations have been presented at XXXIst Rencontres de Moriond: "Four-jet events in L3", presented by R. Faccini, and "Four-jet events in OPAL", presented by H.C. Schultz-Coulon.

[4] DELPHI Collaboration, P. Aarnio et al., *Nucl. Instr. and Meth.* **A303** (1991) 233.

[5] DELPHI Collaboration, P. Abreu et al., *Nucl. Instr. and Meth.* **A378** (1996) 57.

[6] V. Chabaud et al., *Nucl. Instr. and Meth.* **A368** (1996) 314.

[7] T.Sjostrand, Comp. Phys. Comm. **82** (1994) 74;
T.Sjostrand, CERN-TH.7112/93.

[8] J.E. Campagne and R. Zitoun, *Z. Phys.* **C43** (1989) 469.

[9] S. Bethke et al., *Nucl. Phys.* **B370** (1992) 310.

[10] JADE Collaboration, W. Bartel et al., *Z. Phys.* **C33** (1986) 23.

[11] Mark II Collaboration, R. Jacobsen et al. *Phys. Rev. Lett.* **67** (1991) 3347.

[12] H. Baer *et al.*, in *Physics at LEP*, edited by J. Ellis and R. Peccei, CERN Report 86-02, vol. 1, p.297; S. Komamiya, *Phys. Rev.* **D38** (1988) 2158; E. Accomando *et al.*, in *Physics at LEP2*, edited by G. Altarelli, T. Sjostrand and F. Zwirner, CERN Report 96-01, vol. 1, p.351.

[13] R.A. Fisher, The use of multiple measurements in taxonomic problems, Annals of Eugenics, vol.7 (1936); M.G. Kendall and A. Stuart, The advanced theory of statistics, vol.3, 1966, GRIFFIN ed., London.

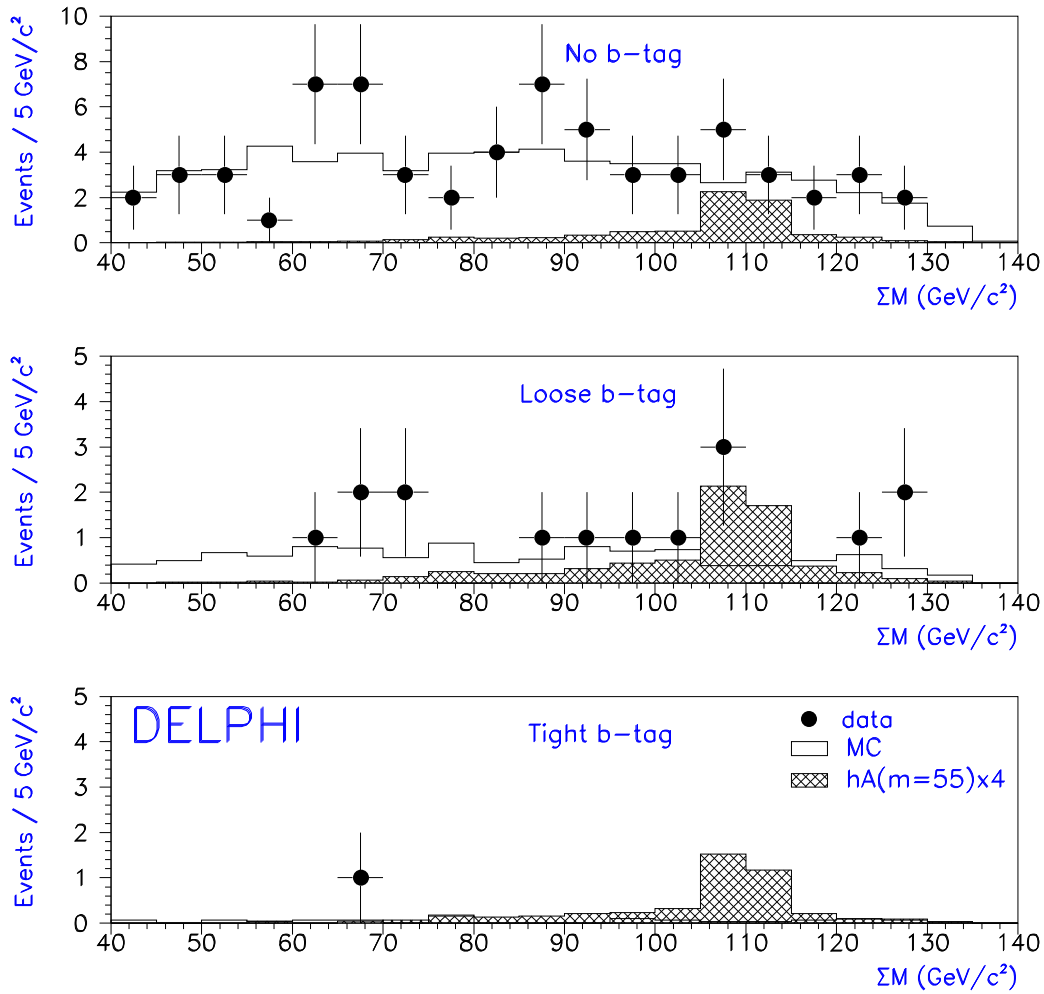[14] N.J. Kjaer, Ph.D. thesis, Niels Bohr Institute, Copenhagen, 1991.

Figure 1: hA analysis: Distribution of the sum of the di-jet masses $\Sigma M$ for data, simulated background, and simulated signal (multiplied by a factor four) for three levels of $b$-tagging.
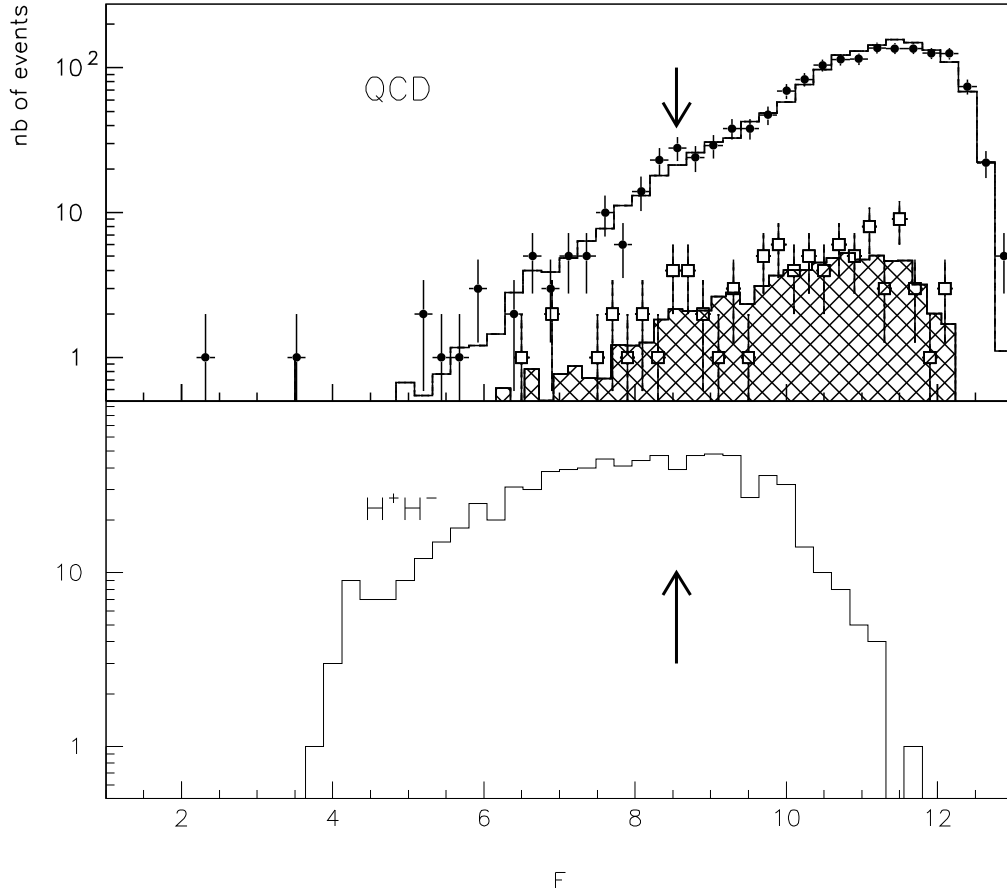
Figure 2: $e^+e^- \rightarrow H^+H^-$ analysis : distribution of the multidimensional function F used in the analysis. The arrow indicates the cut applied. The dots (squares) with error bars show the preselected hadronic (four-jet) data. The histograms show the simulated $e^+e^- \rightarrow f\bar{f}(n\gamma)$ events (upper plot, with the four jet selection shaded) and signal events (lower plot). The signal events shown were generated with $m_{H+} = 44\,\text{GeV}/c^2$ and no width was given to the $H^+$ ; the distribution is plotted at the hadronic preselection level.
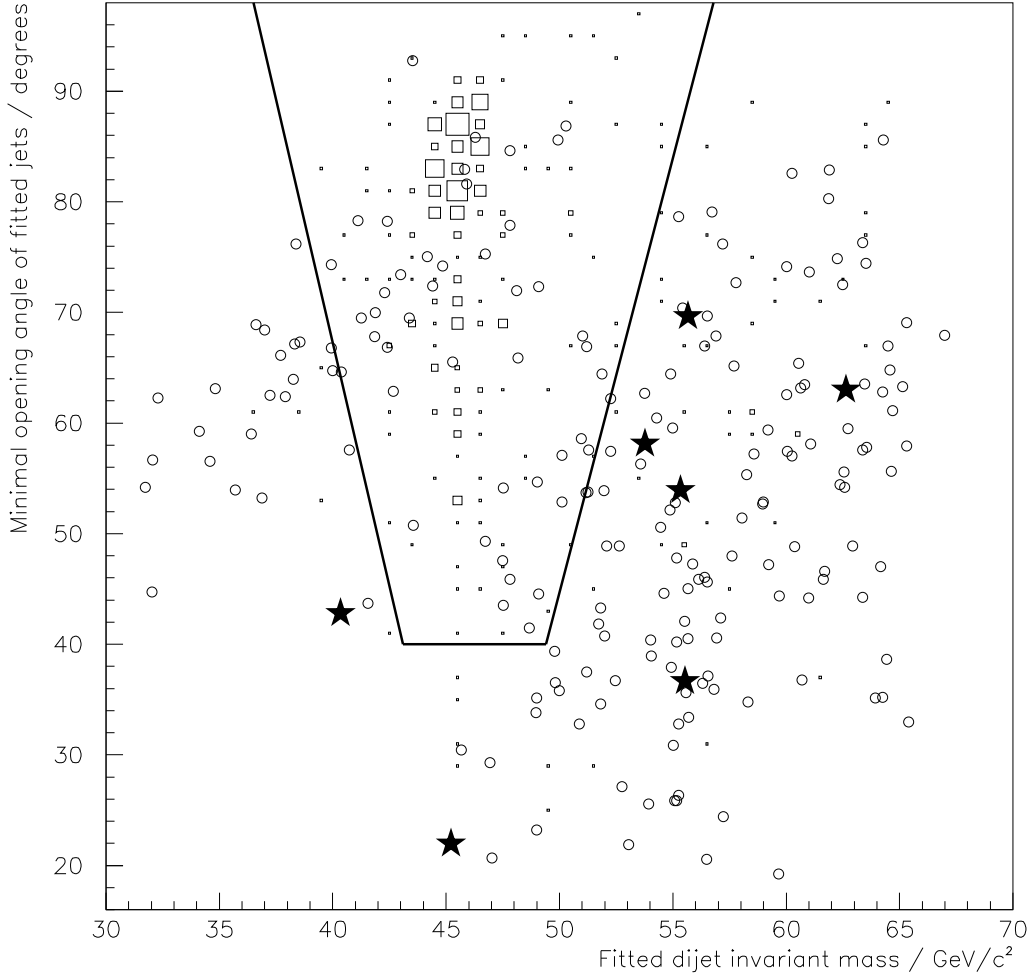
Figure 3: $e^+e^- \to H^+H^-$ analysis : Final cuts on the values of the reconstructed $H^+$ mass and of the minimal angle between any two jets once their momenta have been changed by the kinematic fit. Black stars are the seven events remaining before these cuts. Empty circles are the simulated $e^+e^- \to f\bar{f}(n\gamma)$ events and the square boxes have areas proportional to the number of signal events generated with $m_{H^+} = 46\,\mathrm{GeV}/c^2$. The lines indicate the final cuts.
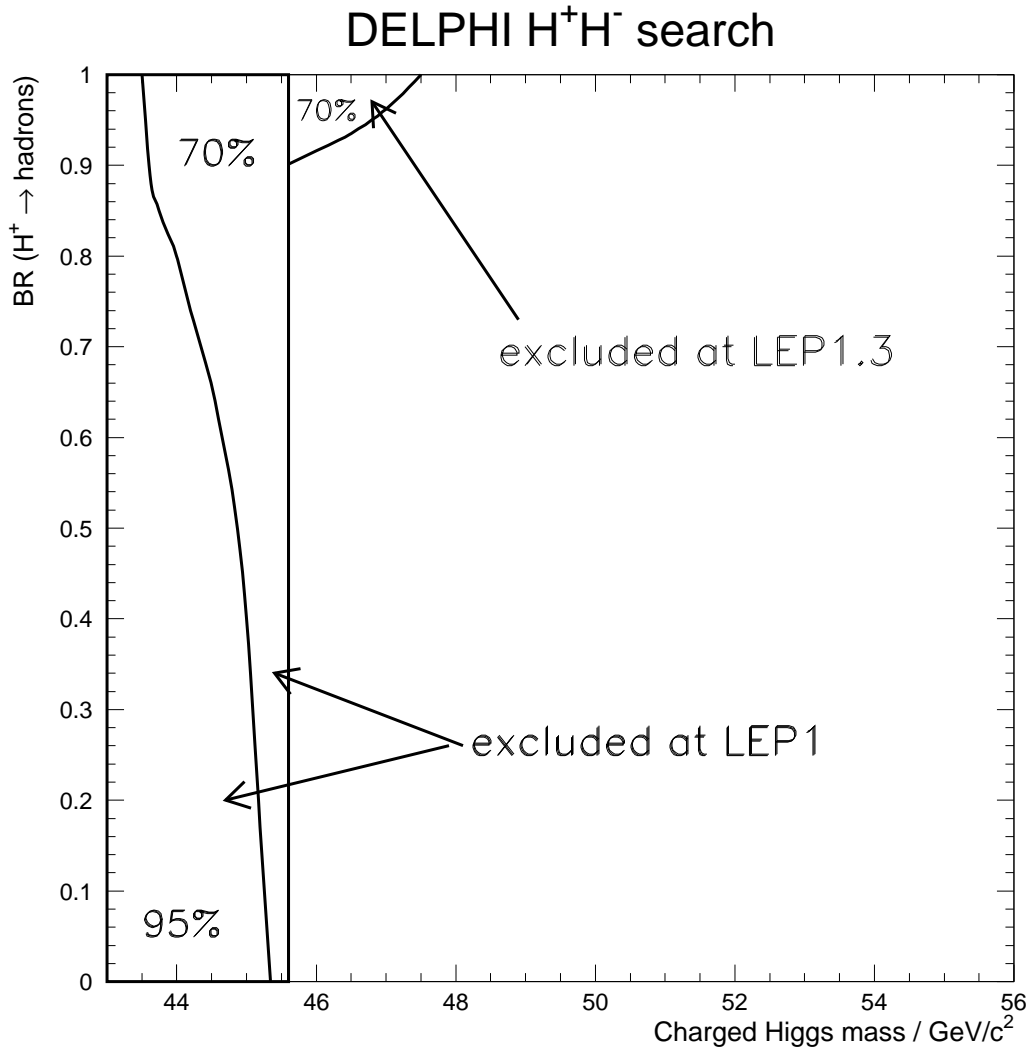
Figure 4: $e^+e^- \to H^+H^-$ analysis : Excluded regions in the $[m_{H^+}, BR(H^+ \to hadrons)]$ plane. On the left are represented the regions excluded at LEP1 (with 70% CL, the kinematic limit was reached; with 95% CL, DELPHI obtained the plotted curve). The upper region was rejected by the present four-jets analysis.
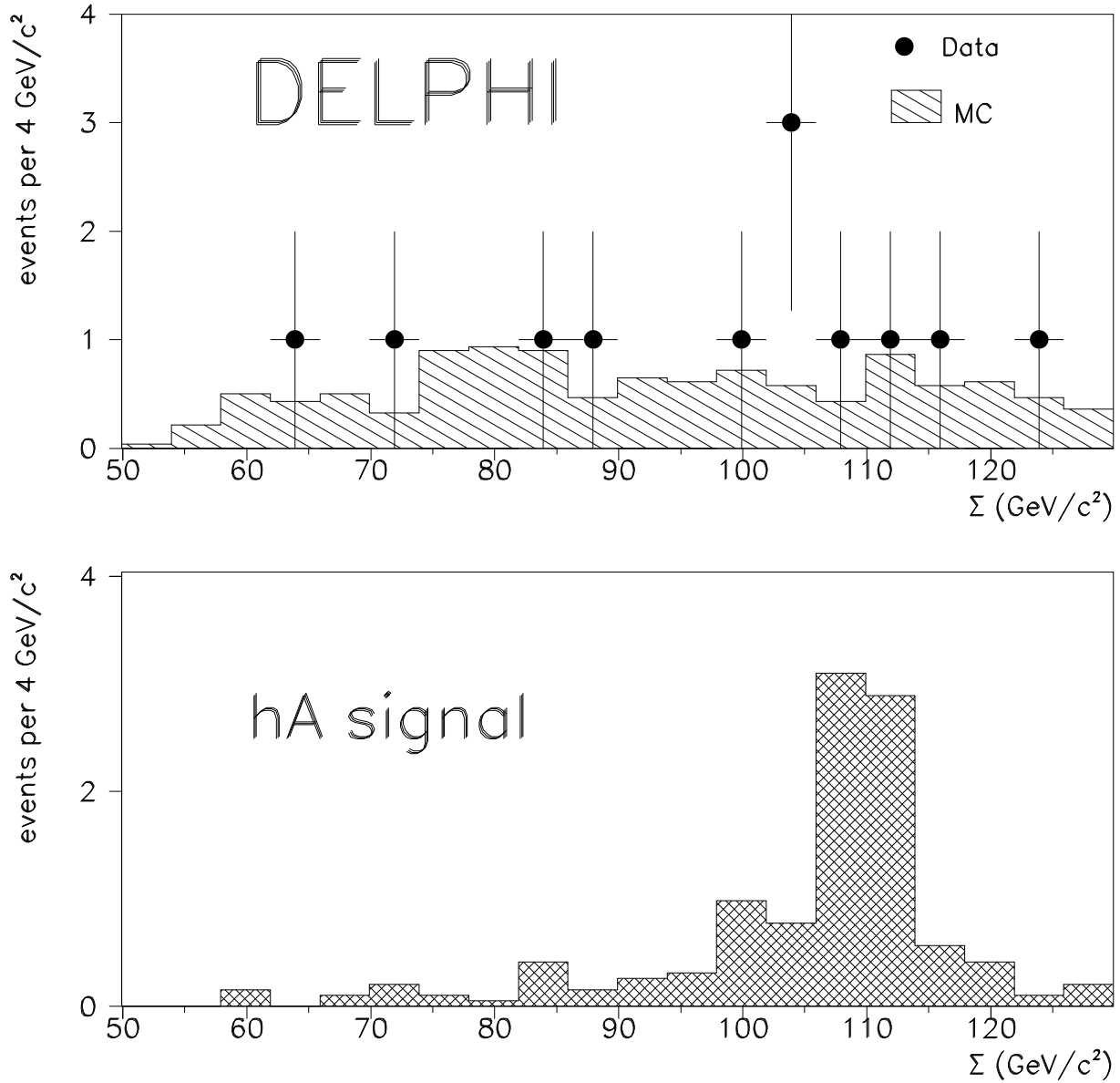
Figure 5: Distribution of sum of di-jet masses $\Sigma M$ for the selected combination after the ALEPH-like cuts for data (dots) and expected standard processes (hatched histogram). As reference, the corresponding distribution for the simulated hA-like signal with $m_h = m_A = 55\,\mathrm{GeV}/c^2$ and zero width and for an arbitrary cross-section ( 4 pb ) is shown below.
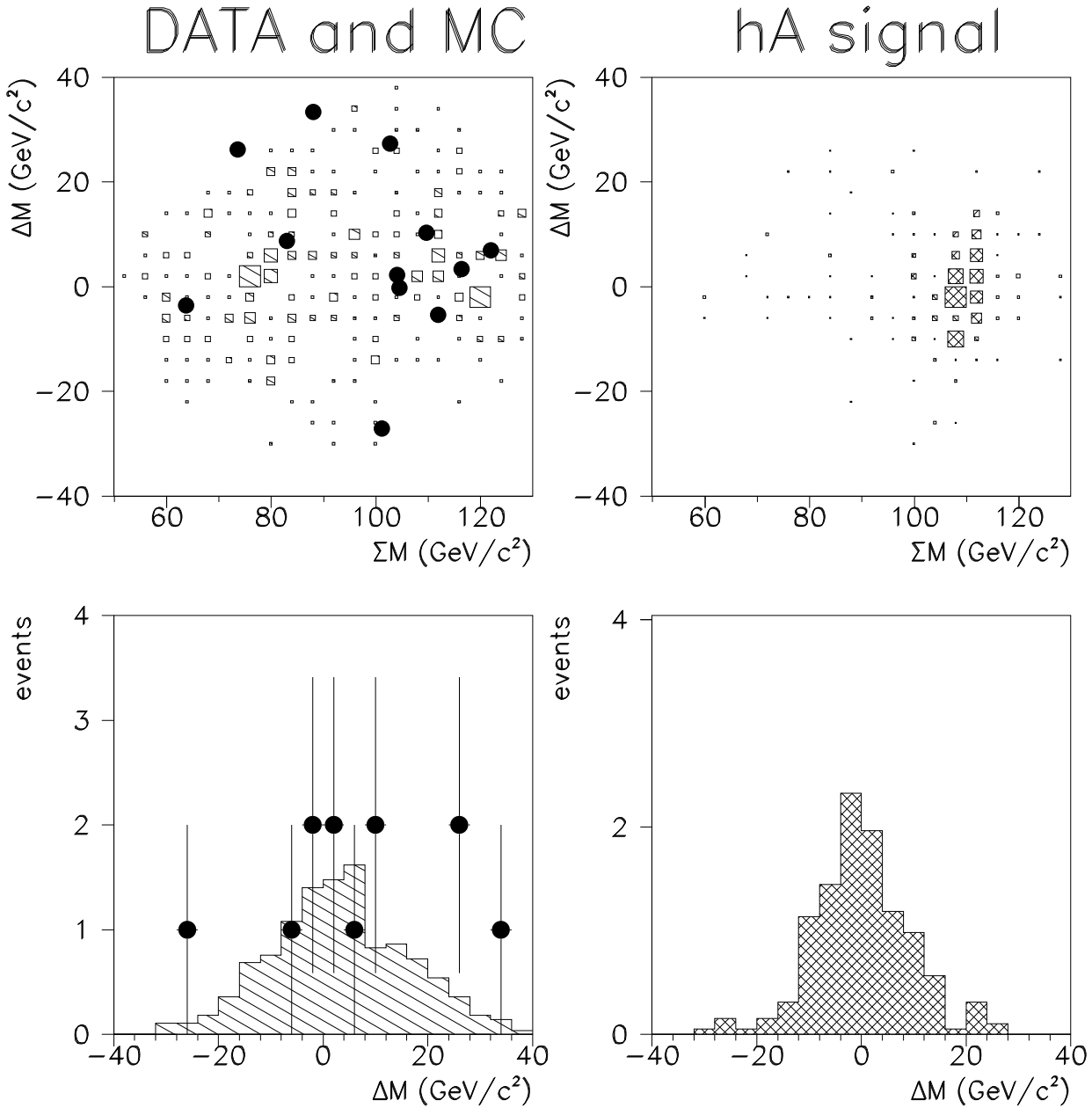
Figure 6: Distribution of the difference $\Delta M = M_{ij} - M_{kl}$ versus the sum $\Sigma M$ of the di-jet masses for the selected pairing. Black dots correspond to data, simple hatching to the Monte Carlo simulation of the background, and crossed hatching to a simulated hA -like signal. The lower plots show the projections onto the $\Delta M$ axis.
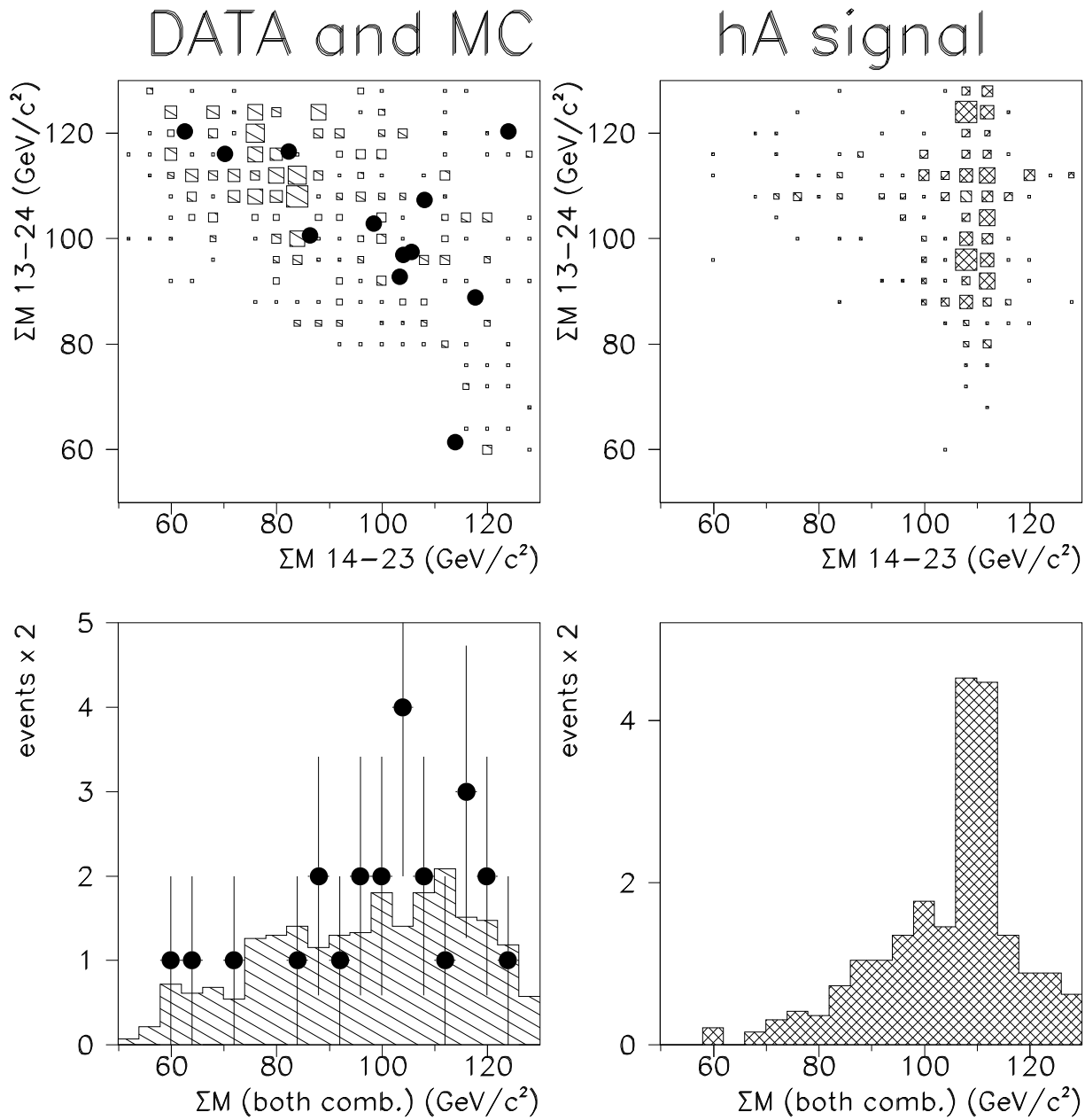
17



Figure 7: Distribution of sum of di-jet masses $\Sigma M$ for the two interesting pairings in each event. Same conventions as in previous figures. Below, both distributions are combined in a single unidimensional plot (with two entries per event, one for each pairing).
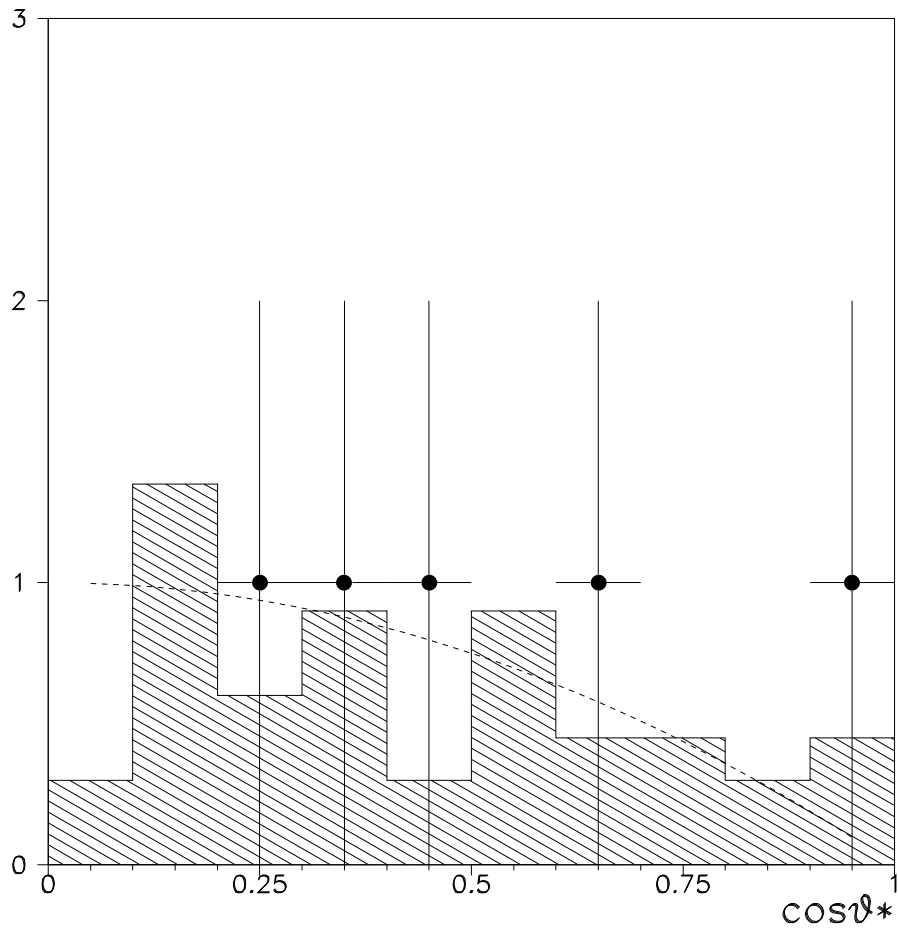
Figure 8: Polar angle of production for a pair of back to back heavy objects each decaying into a di-jet and giving a sum of di-jet masses in the 102–110 $\mathrm{GeV}/c^2$ range in real data (full circles), as expected from QCD background (hatched histogram), and the $\sin^2\theta^*$ distribution (dashed curve) corresponding to production of a pair of scalar particles.
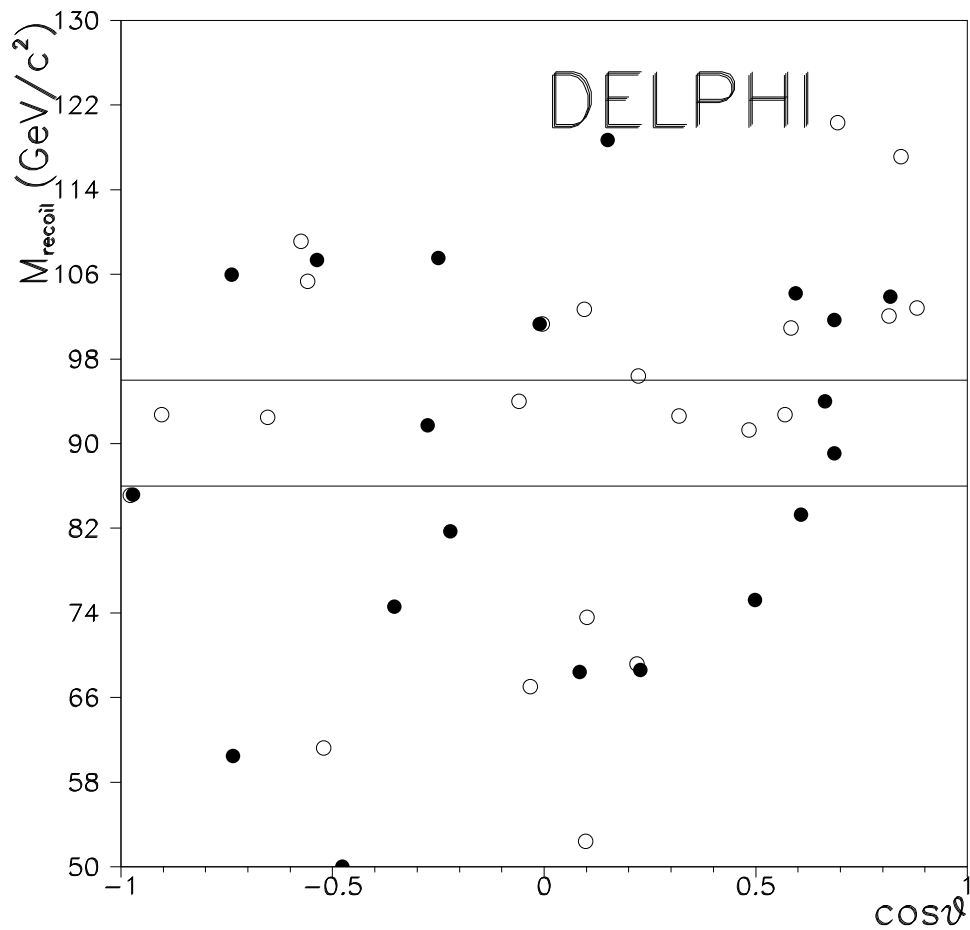
Figure 9: Distribution of the recoil mass for each jet in the selected events versus its polar angle. Black dots correspond to candidate events. Four entries per event (i.e. one per jet) are shown. Radiative events returning to the $Z$ are expected to have a jet with a recoil mass in the horizontal band marked, and with low polar angle ($|\cos \theta|$ above 0.8).